CCFE
CULHAM CENTRE FOR FUSION ENERGY

UK Atomic Energy Authority

UKAEA-CCFE-PR(18)84

A. Fernandez-Caballero, M. Fedorov, J.S. Wrobel,
P.M. Mummery, D. Nguyen

Configurational Entropy in Multicomponent Alloys: Matrix formulation from ab initio based Hamiltonian and application to FCC Cr-Fe-Mn-Ni system

Configurational Entropy in Multicomponent Alloys: Matrix formulation from ab initio based Hamiltonian and application to FCC Cr-Fe-Mn-Ni system

A. Fernandez-Caballero, M. Fedorov, J.S. Wrobel, P.M. Mummery
D. Nguyen

This is a preprint of a paper submitted for publication in Entropy

MDPI

Article

Configurational Entropy in Multicomponent Alloys: Matrix formulation from ab initio based Hamiltonian and application to FCC Cr-Fe-Mn-Ni system

Antonio Fernández Caballero [1,2], Mark Fedorov [3], Jan S. Wróbel [3], Paul M. Mummery [1], and Duc Nguyen-Manh [2,*]

[1] School of Mechanical Aerospace and Civil Engineering, University of Manchester, Manchester M13 9PL, UK
[2] CCFE, United Kingdom Atomic Energy Authority, Abingdon OX14 3DB, UK
[3] Faculty of Materials Science and Engineering, Warsaw University of Technology, Woloska 141, 02-507 Warsaw, Poland
* Correspondence: Duc.Nguyen@ukaea.uk

Academic Editor: name
Version November 7, 2018 submitted to Entropy; Typeset by LaTeX using class file mdpi.cls

Abstract: Configuration entropy is believed to stabilize disordered solid solution phases in multicomponent systems at elevated temperatures over intermetallic compounds by lowering the Gibbs free energy. Traditionally the increment of configuration entropy with temperature was computed by time consuming thermodynamic integration methods. In this work, a new formalism is developed to predict configuration entropy as function of temperature from multi-body cluster probability in a system with arbitrary number of components, K and arbitrary average composition. The formalism uses the principles behind the Cluster Variation Method (CVM) but extends the treatment to arbitrary cluster interaction employed in the Cluster Expansion (CE) technique. The multi-body probabilities are worked out by explicit inversion and direct product of a matrix formulation from point functions in the clusters obtained from symmetry independent correlation functions. The matrix quantities are determined from semi canonical Monte Carlo simulations with Effective Cluster Interactions (ECIs) derived from Density Functional Theory (DFT) calculations. The formalism is applied to analyze the four-body cluster probabilities for the quaternary system Cr-Fe-Mn-Ni. It is shown that for two specific compositions ($Cr_{25}Fe_{25}Mn_{25}Ni_{25}$ and $Cr_{18}Fe_{27}Mn_{27}Ni_{28}$) the high value of probabilities of Cr-Fe-Fe-Fe and Mn-Mn-Ni-Ni are strongly correlated with the presence of the ordering phases $L1_2$-$CrFe_3$ and $L1_0$-MnNi respectively and that are also in excellent agreement with ab initio predictions of these ground state structures. The general formalism is used to investigate configuration entropy as a function of temperature and for 285 different alloy compositions. It is found that our matrix formulation of configuration entropy is in agreement with the result obtained by the thermodynamic integration method. At the high temperature limit, our theoretical prediction for configuration entropy agrees well with random configuration entropy for all compositions of the alloy.

Keywords: Multicomponent; Ab initio; Configuration entropy; Matrix Formulation; Cluster Expansion; Cluster Variation Method; Monte Carlo ; Thermodynamic integration

1. Introduction

Multicomponent systems, termed as High Entropy Alloys (HEAs), are crystalline solids that form predominantly in single phase. These systems were brought to wider attention through the work of Cantor et al [1] and Yeh et al [2]. At or near equiatomic ratio of compositions the configuration

entropy is maximized and given by the formula $S_{config}/R = lnK$ where R the ideal gas constant, and K the total number of different components. It has been proposed to define $K = 4$ as the minimum number of components at or near equiatomic composition for these systems to be called HEAs [3–5].

There are various sources of entropy in a system in addition to configuration entropy including vibration, electronic and magnetic contributions. The co-existence of multiple phases in the equilibrium state of a chemical system with a given overall composition at a specified temperature is found by minimizing the Gibbs free energy of the whole system. When the system undergoes a phase transition of either order-disorder or spinodal decomposition the relative differences of configurational entropy are dominant in comparison to those contributions from vibration and magnetic terms in FeCoCrNi [6] where the relative difference of configuration entropy dominates or is of similar magnitude to vibration entropy. These multicomponent alloys have transition metals Co, Cr, Fe, and Ni that exhibit magnetic behavior and have magnetic phase transitions characterized by Curie temperatures sensitive to concentrations [7].

In general, the formulation of configuration entropy given by the expression $S_{config}/R = lnK$ only holds for disordered alloys with equiatomic composition at temperatures near their melting point. On the other hand at low temperature the lowest free energy structures can be ordered intermetallic phases or partially ordered structures. In the intermediate temperature range there exists short range order, which is related to the nature of the chemical environment of each atomic species containing ordering or segregation preferences specially at low temperatures, because random disordering is favored at the high temperatures. The importance of short-range order was manifested in diffuse X-ray scattering measurements of alloys contained ordered superstructure domains that were seen to significantly affect electrical resistivity properties [8,9], and also influence on the strengthening by hindering dislocation motion [10] in concentrated alloys. Recently, it has been demonstrated how short-range order can be predicted from ab initio based Hamiltonians in combination with Monte Carlo simulations [11] in multicompoment Mo-Nb-Ta-V-W system. The study predicted that strong SRO parameter may lead to the formation of Mo-Ta ordering in the B2 structure after quenching down from temperatures as high as $3,000K$. HEAs such as $Al_{1.3}$CoCrCuFeNi have been reported to be susceptible to complex phase transitions including segregation, precipitation, chemical ordering and spinodal decomposition into a complex microstructure containing regions of BCC, FCC and B2 phases [12]. Physical models have been successfully applied to predict the formation of these phases on the basis of the average number of valence electrons [13].

The prediction of equilibrium thermodynamic properties (free energies, and phase diagrams) is one of the goals of computational materials science. Lattice statistical models involving an Ising-like Hamiltonian developed from ab initio enthalpies of mixing have become an important tool in the computation of the thermodynamic properties of alloy systems. In particular, the cluster expansion (CE) method [14] expands the Hamiltonian into contributions from an optimized set of clusters, each term weighted by Effective Cluster Interactions (ECI). The thermodynamic properties at temperature are obtained from the ECI by computing the free energies from either Monte Carlo methods or the Cluster Variation Method (CVM).

The CVM expresses the free energy in terms of enthalpies of mixing and configuration entropies as a functional of the temperature dependent correlation functions; the free energy value is found at any given temperature by minimizing the free energy from variational principles. The correlation function parameters in terms of which configuration entropy and enthalpy of mixing are expressed grow exponentially with component number K and size of the maximal cluster ω. Due to this, the CVM has been commonly applied to clusters consisting of four sites in a regular tetrahedron or the so-called tetrahedron-octahedron in the FCC lattice [15,16], or the four sites in a irregular tetrahedron in the BCC lattice [17]. It is generally accepted that the Monte Carlo method is more accurate, but the calculations are time consuming due to the need of many passes to obtain free energies at any given temperature from the disordered high temperature configuration. A hybrid approach taking

the Monte Carlo calculated correlation functions at temperature and computing the configuration entropy value from analytic CVM expression has been used to improve the accuracy of the CVM to that of time-consuming thermodynamic integration. This method has been applied to FCC systems in the 13 sites cluster, which consist of a lattice point and its twelve first nearest neighbors, and the 14 sites cluster approximation [18]. However, the analytic expressions for the configuration entropy reported in the literature do not often match those clusters used for the CVM. In this work we close this gap by providing a methodology to develop analytic expressions for configuration entropy matching the clusters from the CE Hamiltonian. We apply our method to CrFeMnNi HEA to arbitrary alloy composition. In particular, the composition $Cr_{18}Fe_{27}Mn_{27}Ni_{28}$ has been used recently to design radiation tolerant materials for advanced nuclear reactor systems. This HEA has been studied for advanced nuclear applications in preference to Cantor's alloy [1] due to the removal of Co, which can cause activation by transmutation of ^{60}Co isotope in nuclear reactors [19].

This paper is organized as follows: In the section 2, a new matrix formulation within the cluster expansion method is introduced that links cluster correlation functions obtained from Monte Carlo calculations to multi-body probabilities. Notation is developed to treat as general as possible arbitrary cluster sizes, ω, number of components, K, and temperature. In section 3, our general method is illustrated to calculate four-body cluster probabilities as a function of temperature for the two specific compositions of equiatomic $Cr_{25}Fe_{25}Mn_{25}Ni_{25}$ and also the composition $Cr_{18}Fe_{27}Mn_{27}Ni_{28}$ from [19]. In section 4, the general expression for configuration entropy is dicussed for an arbitrary alloy composition at two temperatures 1000 and 3000 K. The changes in configuration entropy are attributed to the lowering of the probabilities of the phases that are most stable at low temperatures and the complementary tendency towards disordered random solution of the alloy at the average composition given. The main conclusions of this work are given in section 5.

2. Methods

2.1. Matrix formulation of cluster expansion

Let us consider an alloy system with arbitrary number, K, of components and crystalline lattice symmetry, in which the disordered phase is described by space group, G. The CE Hamiltonian at $T = 0$ K of the alloy can be found from enthalpies of mixing, $\Delta H_{DFT}^{Mixing}[\vec{\sigma}]$, of derivative alloy structures [14,20] denoted by varying length arrays of spin-like variables $\vec{\sigma}_i$ taking values from 0 to $K-1$. In general a derivative structure of the alloy has non-zero atomic concentrations for each of $p = 1, .., K$ different chemical elements forming it i.e. $x[\vec{\sigma}]_p \neq 0$. For each member structures the reference energy in the calculation of the enthalpy of mixing is the pure element total energy, $E_{total}[p]$, in the same crystallographic symmetry. The alloy enthalpy of mixing is defined as follows:

$$\Delta H_{DFT}^{Mixing}[\vec{\sigma} \equiv \{\sigma_1, \sigma_2, \cdots\}] = E_{total}[\vec{\sigma} \equiv \{\sigma_1, \sigma_2, \cdots\}] - \sum_{p=1,..,K} x_p[\vec{\sigma} \equiv \{\sigma_1, \sigma_2, \cdots\}] E_{total}[p] \quad (1)$$

The enthalpies of mixing are calculated from the total energies $E_{total}[\vec{\sigma}]$ and $E_{total}[p]$ of alloy and pure element, respectively, by density functional theory (DFT) for the underlying lattice. In the CE the $\Delta H_{DFT}^{mixing}[\vec{\sigma}]$ of an arbitrary structure $\vec{\sigma}$ is expanded into a sum of reference clusters, $\Delta H_{CE}^{Mixing}[\vec{\sigma}]$.

$$\Delta H_{CE}^{Mixing}[\vec{\sigma} \equiv \{\sigma_1, \sigma_2, \cdots\}] = \sum_{\omega,n,(s)} m_{\omega,n}^{(s)} J_{\omega,n}^{(s)} \langle \Gamma_{\omega',n'}^{(s')}[\vec{\sigma} \equiv \{\sigma_1, \sigma_2, \cdots\}] \rangle_{\omega,n,(s)} \quad (2)$$

In Eq. 2 each reference cluster is characterized by three labels ω, n and (s). The label ω denotes the total number sites; n is an auxiliary label that refers to highest order coordination shell contained in the reference cluster and finally the label $(s) = (j_1, j_2, \cdots, j_\omega)$, denotes decoration of cluster by point functions with dimension equal to ω and j_i taking values $0, ..., K-1$. For each reference cluster,

an effective cluster interaction (ECI) $J^{(s)}_{\omega,n}$, and the multiplicity per lattice site, $m^{(s)}_{\omega,n}$ are associated. The term $\langle \Gamma^{(s')}_{\omega',n'}[\vec{\sigma}] \rangle_{\omega,n,(s)}$ used in the definition of enthalpy of mixing in Eq. 2 is the thermally averaged cluster correlation function over all clusters $\omega', n', (s')$ which are equivalent to a space group symmetry element of the disordered phase within the reference decorated cluster defined by $\omega, n, (s)$. Overall the triple product of multiplicity, ECI and correlation function, $m^{(s)}_{\omega,n} J^{(s)}_{\omega,n} \langle \Gamma^{(s')}_{\omega',n'}[\vec{\sigma}] \rangle_{\omega,n,(s)}$ gives the energetic contribution per lattice site of the reference cluster ω, n and (s) to the enthalpy of mixing of the particular structure configuration given by $\vec{\sigma}$.

The correlation function is defined as the product of point functions evaluated over the system, and its average is given by the following formula:

$$\begin{aligned} \langle \Gamma^{(s')}_{\omega',n'}[\vec{\sigma}] \rangle_{\omega,n,(s)} &= \langle \gamma_{j_1,K}[\sigma_1] \gamma_{j_2,K}[\sigma_2] \cdots \gamma_{j_\omega,K}[\sigma_\omega] \rangle \\ &= \frac{1}{\Omega[\omega,n]} \sum_{u=1}^{\Omega[\omega,n]} \gamma_{j_1,K}[\sigma_{\overrightarrow{(\omega,n)}_{u_1}}] \gamma_{j_2,K}[\sigma_{\overrightarrow{(\omega,n)}_{u_2}}] \cdots \gamma_{j_\omega,K}[\sigma_{\overrightarrow{(\omega,n)}_{u_\omega}}] \end{aligned} \tag{3}$$

where the point function can be determined following [14] as:

$$\gamma_{j,K}[\sigma_i] = \begin{cases} 1 & \text{if } j = 0\,, \\ -\cos\left(2\pi \lceil \frac{j}{2} \rceil \frac{\sigma_i}{K}\right) & \text{if } j > 0 \text{ and odd}, \\ -\sin\left(2\pi \lceil \frac{j}{2} \rceil \frac{\sigma_i}{K}\right) & \text{if } j > 0 \text{ and even}, \end{cases} \tag{4}$$

In Eq. 3 the correlation function of the system is averaged over the arbitrary crystal structure of the alloy system with configuration $\vec{\sigma}$ over all the set of $\Omega[\omega, n]$ clusters, $\{\overleftrightarrow{(\omega,n)}_u\}_{u=1,2,\cdots,\Omega[\omega,n]}$ where each cluster labeled by u contains ω sites, each site denoted by the vector, $\overrightarrow{(\omega,n)}_{u_i}$. The i-union of the ω vectors, $\overrightarrow{(\omega,n)}_{u_i}$, composes the cluster of vectors, $\left(\overrightarrow{(\omega,n)}_{u_1}, \overrightarrow{(\omega,n)}_{u_2}, \cdots, \overrightarrow{(\omega,n)}_{u_\omega}\right) \equiv \overleftrightarrow{(\omega,n)}_u$. The $u_1, u_2, \cdots, u_\omega$ are numeric labels referring to the values taken by variable u in Eq. 3 that serve to enumerate the vectors making up the u cluster of vectors $\{\overleftrightarrow{(\omega,n)}_u\}$. The clusters $\overleftrightarrow{(\omega,n)}_u$ are symmetrically equivalent to the reference cluster (ω, n) sites by a symmetry operation and that are enumerated by an index taking values $1, 2, \cdots, \Omega[\omega, n]$. $\Omega[\omega, n]$ is defined as the number of times the reference cluster (ω, n) is contained in a structural configuration which can be obtained from Monte Carlo simulation. The sites in the cluster $\{\overleftrightarrow{(\omega,n)}_u\}$ can allocate all of the possible decoration values $\in (s)$ which we express as $(s) = (j_1, j_2, \cdots, j_\omega)$. These integer indexes corresponding to the decorated cluster are parameters for the point functions in Eq. 4.

For an arbitrary ω-sites cluster and K components, the number of ω-tuples formed with integer entries running from $0 \cdots K-1$ can be calculated. For $\omega = 2$, the formula calculates the number of symmetrically unique decorations (s) for a two-point cluster $\langle \Gamma^{(s')}_{\omega',n'}[\vec{\sigma}] \rangle_{\omega=2,n,(s)}$ and K component alloy system reduces to $(K+1)K/2$ [11], where K is the number of components. For higher order cluster, the total number of decorations depend on the cluster coordinates and the space group symmetry G of the high temperature disordered phase i.e. FCC or BCC and can not be simply expressed in terms of K (in general there could be less than $\binom{\omega+K-1}{K-1} = \frac{(\omega+K-1)!}{(K-1)!(\omega)!}$ number of symmetrically unique correlation functions). ATAT [14] numerically works out all the number of symmetrically unique decorated clusters $\omega', n', (s')$ equivalent to $\omega, n, (s)$ and uses one correlation function per set of equivalent decorated clusters $\langle \Gamma^{(s')}_{\omega',n'}[\vec{\sigma}] \rangle_{\omega,n,(s)}$. For convenience in notation, from now on we will use $\langle \Gamma^{(s)}_{\omega,n}[\vec{\sigma}] \rangle = \langle \Gamma^{(s')}_{\omega',n'}[\vec{\sigma}] \rangle_{\omega,n,(s)}$. In general, two decorations (s) and (s') are symmetrically equivalent if there is at least one element in the space group symmetry $g \in G$ that

transforms the sites $\{\vec{\tau}_1, \vec{\tau}_2, \cdots, \vec{\tau}_\omega\} \subset (\omega, n)$ into $\{\vec{\tau}_{g[1]}, \vec{\tau}_{g[2]}, \cdots, \vec{\tau}_{g[\omega]}\} \subset (\omega, n)$ as the permutation connecting the decorations $(s) = (1, 2, \cdots, \omega) \subset \{(s)_{(\omega,n)}\}$ and $(s') = (g[1], g[2], \cdots g[\omega]) \subset \{(s)_{(\omega,n)}\}$. This is given by following equation:

$$g\{\vec{\tau}_1, \vec{\tau}_2, \cdots, \vec{\tau}_\omega\} = \{\vec{\tau}_{g[1]}, \vec{\tau}_{g[2]}, \cdots, \vec{\tau}_{g[\omega]}\} \tag{5}$$

With the symmetry relations between decorations (s) and (s') in any given cluster, we are able to retrieve all K^ω possible ω tuples from the set of unique symmetries corresponding to an ω cluster in ATAT [14]. The point functions $\gamma_{j,K}[\sigma_i]$ used to define the general correlation functions are related to the multi-body cluster probabilities (see below in Eq. 9) by direct products of a linear [21] transformation τ_K

$$(\tau_K)_{ji} \equiv \gamma_{j,K}[\sigma_i] \tag{6}$$

where the new matrix τ is constructed from these point functions,$\gamma_{j,K}[\sigma_i]$. It can be trivially shown that the inverse of Van der Monde matrices with complex entries equal to roots of unity, is its complex conjugate one. The inverse of the τ_K matrix can be obtained from the complex conjugate matrix of τ_K by taking the real and imaginary part and riffling their rows. Fom Eq. 4, the following expression results for a system with K components:

$$(\tau_K^{-1})_{ij} = \begin{cases} \frac{1}{K} & \text{if } j = 0\,, \\ -\frac{2}{K}\cos\left(2\pi\lceil\frac{j}{2}\rceil\frac{\sigma_i}{K}\right) & \text{if } j > 0 \text{ and } j-1 < K \text{ and j odd}, \\ -\frac{2}{K}\sin\left(2\pi\lceil\frac{j}{2}\rceil\frac{\sigma_i}{K}\right) & \text{if } j > 0 \text{ and j even}, \\ -\frac{1}{K}\cos\left(2\pi\lceil\frac{j}{2}\rceil\frac{\sigma_i}{K}\right) & \text{if } j-1 = K \text{ and j odd}, \end{cases} \tag{7}$$

The size of τ_K matrix is KxK, where K is the number of components. It is convenient to perform the matrix multiplications with all K^ω decorations formed from ω-tuples with integer elements running from 0 to K-1. In particular for the case of four component $K = 4$ these matrices τ become by applying Eqs. 4 and 7 for the inverse τ_K^{-1}:

$$\tau_4 = \begin{pmatrix} 1 & 1 & 1 & 1 \\ -1 & 0 & 1 & 0 \\ 0 & -1 & 0 & 1 \\ -1 & 1 & -1 & 1 \end{pmatrix} \qquad \tau_4^{-1} = \frac{1}{4}\begin{pmatrix} 1 & -2 & 0 & -1 \\ 1 & 0 & -2 & 1 \\ 1 & 2 & 0 & -1 \\ 1 & 0 & 2 & 1 \end{pmatrix} \tag{8}$$

We duplicate the symmetrically unique decorations (s) whenever two decorations are connected by symmetry of the disordered structure. For relating two equivalent decorations we find it convenient to use a permutation representation of the space group operator as permutations of ω-site tuples. We use the property of invariance of the cluster expansion to obtain probability distributions from correlation functions [22]. As a consequence of the compact formalism and by using Eqs. 4 and 7, the expression of correlation functions can be rewritten into a matrix form:

$$\langle \Gamma_{\omega,n}^{(ij\cdots)}[\vec{\sigma}]\rangle = \sum_{\forall[(pq\cdots)]}^{K^\omega} \gamma_{i,K}[\vec{\sigma}_p]\gamma_{j,K}[\vec{\sigma}_q]\cdots y_{\omega,n}^{(pq\cdots)}[\vec{\sigma}] \equiv \overbrace{(\tau_K \otimes \cdots \otimes \tau_K)}^{\omega}{}_{ij\cdots,pq\cdots} y_{\omega,n}^{(pq\cdots)}[\vec{\sigma}] \tag{9}$$

With the aid of the matrix formulation from Eq. 9 and the generalized form of the inverse matrix τ_K^{-1} in Eq. 7, one can express the ω-cluster probabilities into a matrix form:

$$y_{\omega,n}^{(pq\cdots)}[\vec{\sigma}] = \overbrace{(\tau_K^{-1} \otimes \cdots \otimes \tau_K^{-1})}^{\omega}{}_{pq\cdots,ij\cdots} \langle \Gamma_{\omega,n}^{(ij\cdots)}[\vec{\sigma}]\rangle \tag{10}$$

where we have used of the notation for direct product of matrices $\overbrace{(\tau_K^{-1} \otimes \cdots \otimes \tau_K^{-1})}^{\omega}{}_{pq\cdots,ij\cdots} = (\tau_K)_{p,i}(\tau_K)_{q,j}\cdots$. And we also implied summation over repeated indexes on the right hand side of Eq. 10. Note that the size of these matrices increases exponentially with cluster size ω, K^ωxK^ω; in particular for $\omega = 4$ the matrices have 256x256 entries. The cluster probabilities are normalized as expressed in Eq. 11

$$\sum_{\forall[(pq\cdots)]}^{K^\omega} y_{\omega,n}^{(pq\cdots)}[\vec{\sigma}] = 1 \tag{11}$$

As a consequence of the normalization of the cluster probabilities, it is possible to separate probabilities of the decorated sub-clusters from the probabilities of the maximal cluster by partial summations over all possible decorations for the sites that belong to the maximal cluster ω, n but not the i-th sub-cluster ω_i, n_i.

$$\sum_{(pq\cdots)\in\{[(pq\cdots)_{\omega_i,n_i}]\}} y_{\omega_i,n_i}^{(pq\cdots)}[\vec{\sigma}] = y_{\omega,n}^{(pq\cdots)}[\vec{\sigma}] \tag{12}$$

From Eq. 10 and for the case with ω=2, it follows the generalized expression for SRO of species p and q at the nth shell, $\alpha_{2,n}^{(pq)}[\vec{\sigma}]\,(\,p \neq q\,)$, can be interpreted as the tendency to order or segregate species p and q with respect the disordered random probability given by the product of their elemental, p, bulk concentration $x_p[\vec{\sigma}]$. For the four component Cr-Fe-Mn-Ni system, there are 6 chemically distinct SRO parameters: $\alpha_{2,n}^{(01)}[\vec{\sigma}]$ for Cr-Fe, $\alpha_{2,n}^{(02)}[\vec{\sigma}]$ for Cr-Mn, $\alpha_{2,n}^{(03)}[\vec{\sigma}]$ for Cr-Ni, $\alpha_{2,n}^{(12)}[\vec{\sigma}]$ for Fe-Mn, $\alpha_{2,n}^{(13)}[\vec{\sigma}]$ for Fe-Ni, and $\alpha_{2,n}^{(23)}[\vec{\sigma}]$ for Mn-Ni. The SRO allows a quantitative description of the interactions between atoms as a function of temperature to predict order-disorder transition temperatures [11,23]. In particular the matrix formalism from Eqs. 7 and 10 allows one to generalize the SRO treatment for an arbitrary number of components, K:

$$y_{2,n}^{(pq)}[\vec{\sigma}] = x_p[\vec{\sigma}]x_q[\vec{\sigma}](\,1 - \alpha_{2,n}^{(pq)}[\vec{\sigma}]) \tag{13}$$

2.2. Configuration entropy in the matrix formulation

In general, a thermodynamical system in state $\vec{\sigma}$ and with enthalpy of mixing given by the CE Hamiltonian $\Delta H_{CE}^{Mixing}[\vec{\sigma}]$ is described by a set of symmetry unique probability distributions $y_{\omega,n}^{(pq\cdots)}[\vec{\sigma}]$ characterized by decorations of a chosen maximal ω, n cluster. In practice the chosen maximal cluster ω, n contains few points (for the tetrahedron approximation, four nearest neighbour cluster within the CVM [15]). As a mean field approximation [21], the CVM can be rationalized as a factorization of the probability distributions of the ω, n maximal cluster into integer powers $\eta_{\omega_1,n_1}, \eta_{\omega_2,n_2}\cdots, \eta_{\omega_{s[\omega,n]},n_{s[\omega,n]}}$ of the probability distributions of the sub-clusters $(\omega_i, n_i) \subseteq (\omega, n); i = 1,\cdots,[\omega, n]$ [24] with decorations $(pq\cdots)_{\omega_i,n_i}$ corresponding to the components $(pq\cdots)_{\omega_i,n_i}$ of all decorations $(pq\cdots) \in \{(pq\cdots)_{(\omega,n)}\}$ occupied by sites of the ω_i, n_i sub-cluster

$$y_{\omega,n}^{(pq\cdots)}[\vec{\sigma}] = (y_{\omega_1,n_1}^{(pq\cdots)_{\omega_1,n_1}}[\vec{\sigma}])^{\eta_{\omega_1,n_1}}(y_{\omega_2,n,2}^{(pq\cdots)_{\omega_2,n_2}}[\vec{\sigma}])^{\eta_{\omega_2,n_2}}\cdots(y_{\omega_{[\omega,n]},n_{[\omega,n]}}^{(pq\cdots)_{\omega_{[\omega,n]},n_{[\omega,n]}}}[\vec{\sigma}])^{\eta_{\omega_{[\omega,n]},n_{[\omega,n]}}} \tag{14}$$

The following expression, a consequence of the CVM factorization scheme, can be derived from [24] and is the reason why the disordered configuration at high temperature is reproduced from multi-body probabilities $\sum_{i=1}^{[\omega,n]} \omega_i\eta_{\omega_i,n_i} = -1$. This occurs because at the high temperature limit the CVM probabilities tend to products of composition of the species involved in the decorations of the cluster:

$$y_{\omega_i,n_i}^{(pq\cdots)_{\omega_i,n_i}}[\vec{\sigma}] \underset{T\to\infty}{\rightarrow} \prod_{j=1}^{\omega_i} y_{1,1}^{((pq\cdots)_j)_{\omega_i,n_i}}[\vec{\sigma}] = \prod_{j=1}^{\omega_i} x_{((pq\cdots)_j)_{\omega_i,n_i}}[\vec{\sigma}] \tag{15}$$

where $y_{1,1}^{((pq\cdots)_j)_{\omega_i,n_i}}[\vec{\sigma}] = x_{(pq\cdots)_{\omega_i,n_i}}[\vec{\sigma}]$ is the concentration of the $(pq\cdots)_j$ equal to one of the integers $0, 1, \cdots, K-1$ in the disordered state of the alloy. A natural consequence of the factorization scheme chosen for the CVM multi-body probabilities is that the configuration entropy assumes the formulation

$$S_{\omega,n}[\vec{\sigma}] \equiv \sum_{i=1}^{[\omega,n]} \eta_{\omega_i,n_i} \widetilde{S}_{\omega_i,n_i}[\vec{\sigma}] = \sum_{i=1}^{[\omega,n]} \eta_{\omega_i,n_i} \sum_{\forall[(pq\cdots)_{\omega_i,n_i}]}^{K^{\omega_i}} k_B y_{\omega_i,n_i}^{(pq\cdots)_{\omega_i,n_i}}[\vec{\sigma}] ln(y_{\omega_i,n_i}^{(pq\cdots)_{\omega_i,n_i}}[\vec{\sigma}]) \tag{16}$$

where $\widetilde{S}_{\omega_i,n_i}$, is the entropy contribution to cluster (ω, n) from the sub-cluster (ω_i, n_i):

$$\widetilde{S}_{\omega_i,n_i}[\vec{\sigma}] = \sum_{\forall(pq\cdots)_{\omega_i,n_i}}^{K^{\omega_i}} k_B y_{\omega_i,n_i}^{(pq\cdots)_{\omega_i,n_i}}[\vec{\sigma}] ln(y_{\omega_i,n_i}^{(pq\cdots)_{\omega_i,n_i}}[\vec{\sigma}]) \tag{17}$$

The set of integers $\eta_{\omega_1,n_1}, \eta_{\omega_2,n_2} \cdots, \eta_{\omega_{s[\omega,n]},n_{s[\omega,n]}}$ are the mean field integer coefficients associated with the partition function of the alloy system. In the theory of regular mixtures, the coefficients can be found from the recursive heuristic expression after Kikuchi, [25], Barker [26] and whose formulation was explicitly derived by using group theoretic methods by Gratias et al. [27]. It requires the determination of two quantities: the site multiplicity N_{ω_i,n_i} and the sub-cluster multiplicity N_{ω_i,n_i}^{β}. The site multiplicity can be determined by calculating the number of symmetry operators, $\mathcal{N}_{\omega_i,n_i}$, that stabilize the ω_i, n_i cluster i.e.$g \in G$ such that the application of g into the set of cluster positions $\{\vec{\tau}_1, \vec{\tau}_2, \cdots, \vec{\tau}_\omega\}$ results in a permutation of the set; then $N_{\omega_i,n_i} = \frac{|G|}{|\mathcal{N}_{\omega_i,n_i}|}$ where $|G|$ is the order of the point group associated to the space group G and $|\mathcal{N}_{\omega_i,n_i}|$ is the order of the group $\mathcal{N}_{\omega_i,n_i}$. The sub-cluster multiplicity N_{ω_i,n_i}^{β} is just the frequency of the cluster β that is contained in the cluster ω_i, n_i

$$\eta_{\omega_i,n_i} = -N_{\omega_i,n_i} - \sum_{(\omega_i,n_i)\subset\beta\subseteq(\omega,n)} N_{\omega_i,n_i}^{\beta} \eta_{\beta} \tag{18}$$

In particular the formulation applied to point cluster retrieves the Bragg-Williams approximation for maximal cluster $(\omega = 1, n = 1)$, i.e a site cluster, giving the entropy weight of $\eta_{\omega_1=1_1,n_1=1} = -1$ and for a two body cluster $(\omega = 2, n)$ in the n^{th} coordination shell, we get $\eta_{\omega_2,n_2} = -N_{2,n}$ and $\eta_{\omega_1,n_1} = 2N_{2,n} - 1$, where $N_{2,n}$ is site multiplicity of the cluster $(2, n)$ calculated from the sites in this cluster and the space group G.

This formulation is valid for the CVM method or for the hybrid CE-Monte Carlo method; in the hybrid CE-Monte Carlo technique, the free energy minimization is performed by Monte Carlo technique, and in the process, the Monte Carlo produces the correlation functions for the equilibrium configurations found at each of the temperatures investigated [28]. The hybrid approach uses these correlation functions in the analytic expressions for configuration entropy.

There is an alternative to the hybrid approach for the entropy calculation where the thermodynamic integration method can be used. Here entropy is calculated from the contribution to the specific heat at constant volume, C_{conf} derived from the fluctuations of enthalpy of mixing at temperature values in a fine grid of temperature values:

$$S_{conf}[T] = \int_0^T \frac{C_{conf}}{T'} dT' = \int_0^T \frac{\langle \Delta H_{CE}^{Mixing^2} \rangle - \langle \Delta H_{CE}^{Mixing} \rangle^2}{T'^3} dT' \tag{19}$$

where $\langle \Delta H_{CE}^{Mixing} \rangle^2$ and $\langle \Delta H_{CE}^{Mixing^2} \rangle$ are the square of the mean and mean square enthalpies of mixing, respectively, calculated by averaging over all the MC steps at the accumulation stage for a given temperature. The accuracy of evaluation of configurational entropy depends on the size of temperature integration step and the number of MC steps performed at the accumulation stage [29].

2.3. Computational details

The DFT enthalpies of mixing given by Eq. 1 were calculated from DFT total energies performed using the projector augmented wave (PAW) method [30] implemented in VASP [31–35]. Exchange and correlation were treated in the generalized gradient approximation GGA-PBE [36]. The core configurations of Fe, Cr, Mn and Ni in PAW potentials are [Ar]3d^{7}4s^1, [Ar]3d^{5}4s^1, [Ar]3d^{6}4s^1 and [Ar]3d^{9}4s^1, respectively. Total energies were calculated using the Monkhorst-Pack [37] mesh of 12x12x12 k-point for a four-atom FCC cubic cell. The plane wave cut-off energy used in the calculations was 400 eV. The total energy convergence criterion was set to 10^{-6} eV/cell, and force components were relaxed to 10^{-3} eV/nm. The DFT enthalpies of mixing were fitted into the cluster expansion given by Eq. 2 of the FCC CrFeMnNi system resulting in a minimal cross-validation criterion of 12.95 meV/atom, which is an indicator for the average difference $\Delta H_{DFT}^{Mixing}[\vec{\sigma}] - \Delta H_{CE}^{Mixing}[\vec{\sigma}]$ for all structures $\vec{\sigma}$ of the database employed to perform the cluster expansion. The database of structures for the cluster expansion consisted on 835 structures categorized by the difference of local environments in binaries (structures with two chemical elements: 58 CrFe, 55 CrMn, 77 CrNi, 58 FeMn, 54 FeNi and 52 MnNi), ternaries (structures with three chemical elements: 89 CrFeMn, 85 CrFeNi, 46 FeMnNi, and 66 CrMnNi); and 191 quaternaries CrFeMnNi.

In the semi canonical Monte Carlo calculations performed the temperature range and temperature steps are important. The accuracy of the thermodynamic integration method to calculate configuration entropy generally requires a lower temperature integration step, $\Delta T = 10$ K and also depends on the number of Monte Carlo passes [29]. In particular, we use a cell containing 2048 atoms distributed into a 8x8x8 primitive unit cell, and average compositions for the ensemble given by $Cr_{18}Fe_{27}Mn_{27}Ni_{28}$ and equiatomic $Cr_{25}Fe_{25}Mn_{25}Ni_{25}$. The simulations start at high temperature 3,000 K where the semi canonical potential at the high-temperature limit is given by $k_BTln(4)$ for equiatomic and $-k_BT\{0.18 * ln(0.18) + 2 * 0.27 * ln(0.27) + 0.28 * ln(0.28)\}$ for $Cr_{18}Fe_{27}Mn_{27}Ni_{28}$ [28], and then we integrated numerically the canonical potential in temperature steps of $\Delta T = 10$ K to reach $T = 100$ K for equiatomic and $T = 180K$ for the system with composition $Cr_{18}Fe_{27}Mn_{27}Ni_{28}$, respectively. For thermodynamic integration calculation of configuration entropy, we use theoretical formula 19.

3. Four-body probability functions in fcc Cr-Fe-Mn-Ni alloys

We apply the methods to the FCC CrFeMnNi system to calculate the temperature and composition dependent cluster probability distribution functions and the configuration entropy.

3.1. Cluster Expansion Hamiltonian for FCC CrFeMnNi

The cluster expansion Hamiltonian for the quaternary system CrFeMnNi consists in total of 83 different decorated clusters distributed among 10 different non-decorated clusters: 4 decorated clusters for the point cluster, $\omega = 1, n = 1$; 6 decorated clusters for each pair cluster $\omega = 2, n = 1, \cdots, 6$; 10 decorated clusters for the non-decorated cluster $\omega = 3, n = 1$; 18 decorated clusters for the non-decorated cluster $\omega = 3, n = 2$; and 15 decorated clusters for the non-decorated cluster $\omega = 4, n = 1$. The decoration labels, (s) required to specify the clusters, are listed in Tab. 1. Each non-decorated cluster is defined by the coordinates (specified with respect to the standard Cartesian coordinate system in units of lattice spacing) of the lattice sites that it includes. The decorations define the chemical species allocated to each site in strictly the same order i.e. for $\omega = 2, n = 1$ cluster the

decoration $(2,3)$ means that species 2 is allocated for site with coordinates $(1,1,1)$ and species 3 is allocated for site with coordinates $(1/3,3/2,3/2)$.

Table 1. ω, highest coordination shell n, decoration (s) and coordinates of points in the relevant clusters on FCC lattice. The coordinates are referred to the simple cubic Bravais lattice. Index (s) is the same as the sequence of points in the relevant cluster. The canonical order for decoration indexes, $(s)_i$, is 0,1,2 and 3 is Cr, Fe, Mn and Ni.

ω	n	(s)	Coordinates
1	1	(0)	(1,1,1)
		(1)	
		(2)	
		(3)	
2	1	(1,1)	((1,1,1),(1,3/2,3/2))
		(2,1)	
		(3,1)	
		(2,2)	
		(3,2)	
		(3,3)	
2	2	(1,1)	((1,1,1),(1,1,0))
		(2,1)	
		(3,1)	
		(2,2)	
		(3,2)	
		(3,3)	
2	3	(1,1)	((1,1,1),(2,3/2,3/2))
		(2,1)	
		(3,1)	
		(2,2)	
		(3,2)	
		(3,3)	
2	4	(1,1)	((1,1,1),(2,1,2))
		(2,1)	
		(3,1)	
		(2,2)	
		(3,2)	
		(3,3)	
2	5	(1,1)	((1,1,1),(1,3/2,-1/2))
		(2,1)	
		(3,1)	
		(2,2)	
		(3,2)	
		(3,3)	
2	6	(1,1)	((1,1,1),(2,2,0))
		(2,1)	
		(3,1)	
		(2,2)	
		(3,2)	
		(3,3)	
3	1	(1,1,1)	((1,1,1),(3/2,1,1/2),(1,3/2,1/2))
		(2,1,1)	
		(3,1,1)	
		(2,2,1)	
		(3,2,1)	
		(3,3,1)	
		(2,2,2)	
		(3,2,2)	
		(3,3,2)	
		(3,3,3)	
3	2	(1,1,1)	((1,1,1),(1,3/2,1/2),(1,1,0))
		(2,1,1)	
		(3,1,1)	
		(1,2,1)	
		(2,2,1)	
		(3,2,1)	
		(1,3,1)	
		(2,3,1)	
		(3,3,1)	
		(2,1,2)	
		(3,1,2)	
		(2,2,2)	
		(3,2,2)	
		(2,3,2)	
		(3,3,2)	
		(3,1,3)	
		(3,2,3)	
		(3,3,3)	
4	1	(1,1,1,1)	((1,1,1),(3/2,3/2,1),(3/2,1,1/2),(1,3/2,1/2))
		(2,1,1,1)	
		(3,1,1,1)	
		(2,2,1,1)	
		(3,2,1,1)	
		(3,3,1,1)	
		(2,2,2,1)	
		(3,2,2,1)	
		(3,3,2,1)	
		(3,3,3,1)	
		(2,2,2,2)	
		(3,2,2,2)	
		(3,3,2,2)	
		(3,3,3,2)	
		(3,3,3,3)	

3.2. Semi canonical Monte Carlo simulations

After performing the Monte Carlo simulations for alloy compositions $Cr_{18}Fe_{27}Mn_{27}Ni_{28}$ and equiatomic $Cr_{25}Fe_{25}Mn_{25}Ni_{25}$, we use the correlation functions calculated at each of the temperatures to study the temperature dependent probabilities of decorated clusters corresponding to the equilibrium configuration $[\vec{\sigma}]$ of the Monte Carlo supercell following the formalisms described in

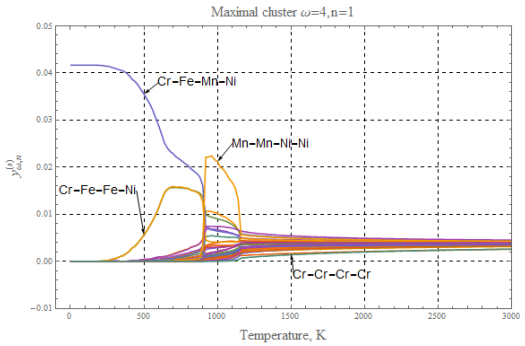

(a) All the four-body probabilities for the equiatomic composition $Cr_{25}Fe_{25}Mn_{25}Ni_{25}$ as a function of temperature.

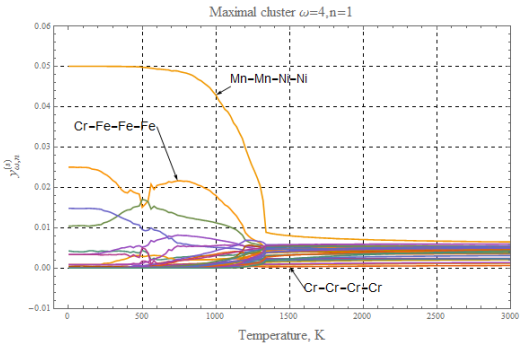

(b) The same as in (a) but for the composition $Cr_{18}Fe_{27}Mn_{27}Ni_{28}$.

Figure 1. Four-body probabilities obtained from the hybrid CE-Monte Carlo calculations.

the Methods. For each non-decorated cluster ω, n and temperature we generate the corresponding τ^{-1} matrices with dimension K^ωxK^ω and a vector formed by all the decorated correlation cluster functions, $\langle \Gamma^{(ij\cdots)}_{\omega,n}[\vec{\sigma}] \rangle$ with dimension K^ω. The Monte Carlo simulations output only the symmetry unique correlation functions (see Tab. 1), which are less than the K^ω required for matrix operation. In order to generate the full set of K^ω from the symmetrically unique correlation functions we devise a set of permutation operators g_i (see Tab. 2) that indicate how an arbitrary decoration ω-tuple of integers is obtained from to the symmetrically unique decorations belonging to the non-decorated cluster or one of its sub-clusters (see the third column of Tab. 2 for identifying the cluster-sub-cluster relation). Tab. 2 contains all the operators necessary to generate cluster probabilities, $y^{(s)}_{\omega,n}$, for any possible decoration, (s), of 9 non-decorated clusters employed in the cluster expansion Hamiltonian.

We use the maximal cluster given by $\omega = 4, n = 1$ for obtaining the four-body temperature dependent configuration probabilities. In particular in Figs. 1 a-b, we plot the 35 symmetrically unique probabilities for the four body maximal cluster defined by the set of lattice sites $((1,1,1),(3/2,3/2,1),(3/2,1,1/2),(1,3/2,1/2))$.

The most probable four-body bonding configurations in the temperature range from 0 to 3000 K for the two alloy systems (the equiatomic $Cr_{25}Fe_{25}Mn_{25}Ni_{25}$ and $Cr_{18}Fe_{27}Mn_{27}Ni_{28}$) are highlighted in Figs. 1 a-b. It should be noted that for both compositions the cluster configuration referred as Cr-Cr-Cr-Cr appears as the least probable of all the cluster configurations.

For the equiatomic composition Cr-Fe-Mn-Ni appears particularly probable at temperatures between 0-900 K, followed by Mn-Mn-Ni-Ni at temperatures between 900-1200 K. Furthermore, in the temperature range 0-900 K, the cluster configuration Cr-Fe-Fe-Ni shows as the second most probable configuration after the Cr-Fe-Mn-Ni configuration. Beyond 1200 K, all of the cluster configuration probabilities tend to the solid solution or random configuration.

For the system with average composition $Cr_{18}Fe_{27}Mn_{27}Ni_{28}$, the cluster probability of decorations given by Mn-Mn-Ni-Ni appears to dominate until 1300 K, where the solid solution or random configuration begins. Furthermore, the second most probable cluster configuration in the temperature range 500-1200 K appears to be Cr-Fe-Fe-Fe.

For each temperature value in the range 0-3000 K the configuration probabilities corresponding to cluster $\omega = 4, n = 1$ are used in Eq. 17 to obtain the quantities $\widetilde{S}_{\omega_i,n_i}[\vec{\sigma}]$. There is one quantity $\widetilde{S}_{\omega_i,n_i}[\vec{\sigma}]$ and a corresponding weight η_{ω_i,n_i} for each of the ω_i, n_i sub-clusters :$\omega = 1, n = 1$, $\omega = 2, n = 1$; $\omega = 3, n = 1$; and $\omega = 4, n = 1$ included in the maximal cluster $\omega = 4, n = 1$. The total configuration entropy, $S_{\omega,n}[\vec{\sigma}]$, is calculated by adding the η_{ω_i,n_i} weighted quantities $\widetilde{S}_{\omega_i,n_i}[\vec{\sigma}]$. By applying the same arguments developed for the cluster $\omega = 4, n = 1$, the total configuration entropy

for each of the 10 different maximal clusters can be calculated. The subclusters and the permutation operators contained in each of the 10 maximal clusters appearing in the cluster expansion are detailed in Tab. 2.

Table 2. Permutation tables for generating the full set of decorations K^{ω} from the set of 83 symmetry unique ones indicated in Tab. 1. The space group of the disordered FCC structure is O_h^5 and the decorations of clusters on which the operators permute sites are indicated in Tab. 1

Maximal cluster	**Permutation operators** $\{g_1, g_2, \cdots\}$	Subcluster $\{\omega_i, n_i\}$	N_{ω_i,n_i}	$N_{\omega,n}^{\omega_i,n_i}$	η_{ω_i,n_i}
$\omega = 1, n = 1$	$\{(1)\}$	$\omega_1 = 1, n_1 = 1$	1	1	-1
$\omega = 2, n = 1$	$\{(1,X),(X,1)\}$	$\omega_1 = 1, n_1 = 1$	1	2	11
	$\{(1,2),(2,1)\}$	$\omega_2 = 2, n_2 = 1$	6	1	-6
$\omega = 2, n = 2$	$\{(1,X),(X,1)\}$	$\omega_1 = 1, n_1 = 1$	1	2	5
	$\{(1,2),(2,1)\}$	$\omega_2 = 2, n_2 = 2$	3	1	-3
$\omega = 2, n = 3$	$\{(1,X),(X,1)\}$	$\omega_1 = 1, n_1 = 1$	1	2	23
	$\{(1,2),(2,1)\}$	$\omega_2 = 2, n_2 = 3$	12	1	-12
$\omega = 2, n = 4$	$\{(1,X),(X,1)\}$	$\omega_1 = 1, n_1 = 1$	1	2	11
	$\{(1,2),(2,1)\}$	$\omega_2 = 2, n_2 = 4$	6	1	-6
$\omega = 2, n = 5$	$\{(1,X),(X,1)\}$	$\omega_1 = 1, n_1 = 1$	1	2	23
	$\{(1,2),(2,1)\}$	$\omega_2 = 2, n_2 = 5$	12	1	-12
$\omega = 2, n = 6$	$\{(1,X),(X,1)\}$	$\omega_1 = 1, n_1 = 1$	1	2	7
	$\{(1,2),(2,1)\}$	$\omega_2 = 2, n_2 = 6$	4	1	-4
$\omega = 3, n = 1$	$\{(1,X,X),(X,X,1),(X,1,X)\}$	$\omega_1 = 1, n_1 = 1$	1	3	-13
	$\{(1,2,X),(2,1,X),(2,X,1),(1,X,2),(X,1,2),(X,2,1)\}$	$\omega_2 = 2, n_2 = 1$	6	3	18
	$\{(1,3,2),(3,2,1),(2,1,3),(3,1,2),(2,3,1),(1,2,3)\}$	$\omega_3 = 3, n_3 = 1$	8	1	-8
$\omega = 3, n = 2$	$\{(1,X,X),(X,X,1),(X,1,X)\}$	$\omega_1 = 1, n_1 = 1$	1	3	-19
	$\{(2,1,X),(1,2,X)\}$	$\omega_2 = 2, n_2 = 2$	1	1	9
	$\{(1,X,2),(2,X,1),(X,1,2),(X,2,1)\}$	$\omega_3 = 2, n_3 = 1$	6	2	18
	$\{(3,1,2),(1,3,2),(1,2,3)\}$	$\omega_4 = 3, n_4 = 2$	12	1	-12
$\omega = 4, n = 1$	$\{(1,X,X,X),(X,X,X,1),(X,X,1,X),(X,1,X,X)\}$	$\omega_1 = 1, n_1 = 1$	1	4	-5
	$\{(X,X,1,2),(X,X,2,1),(1,2,X,X),(2,1,X,X)$ $(X,1,X,2),(X,2,X,1),(2,X,1,X),(1,X,2,X)$ $(1,X,X,2),(2,X,X,1),(X,1,2,X),(X,2,1,X)\}$	$\omega_2 = 2, n_2 = 1$ $\omega_2 = 2, n_2 = 1$ $\omega_2 = 2, n_2 = 1$	6	6	6
	$\{(1,3,2,X),(3,1,X,2),(2,X,1,3),(X,2,3,1)$ $(3,2,1,X),(1,X,3,2),(X,1,2,3),(2,3,X,1)$ $(2,1,3,X),(X,3,1,2),(1,2,X,3),(3,X,2,1)$ $(2,X,3,1),(X,2,1,3),(1,3,X,2),(3,1,2,X)$ $(1,X,2,3),(3,2,X,1),(2,3,1,X),(X,1,3,2)$ $(3,X,1,2),(1,2,3,X),(X,3,2,1),(2,1,X,3)\}$	$\omega_3 = 3, n_3 = 1$ $\omega_3 = 3, n_3 = 1$ $\omega_3 = 3, n_3 = 1$ $\omega_3 = 3, n_3 = 1$ $\omega_3 = 3, n_3 = 1$ $\omega_3 = 3, n_3 = 1$	8	4	0
	$\{(1,4,3,2),(4,1,2,3),(3,2,1,4),(2,3,4,1)$ $(4,3,1,2),(1,2,4,3),(2,1,3,4),(3,4,2,1)$ $(3,1,4,2),(2,4,1,3),(1,3,2,4),(4,2,3,1)$ $(3,2,4,1),(2,3,1,4),(1,4,2,3),(4,1,3,2)$ $(1,2,3,4),(4,3,2,1),(3,4,1,2),(2,1,4,3)$ $(4,2,1,3),(1,3,4,2),(2,4,3,1),(3,1,2,4)\}$	$\omega_4 = 4, n_4 = 1$ $\omega_4 = 4, n_4 = 1$ $\omega_4 = 4, n_4 = 1$ $\omega_4 = 4, n_4 = 1$ $\omega_4 = 4, n_4 = 1$ $\omega_4 = 4, n_4 = 1$	2	1	-2

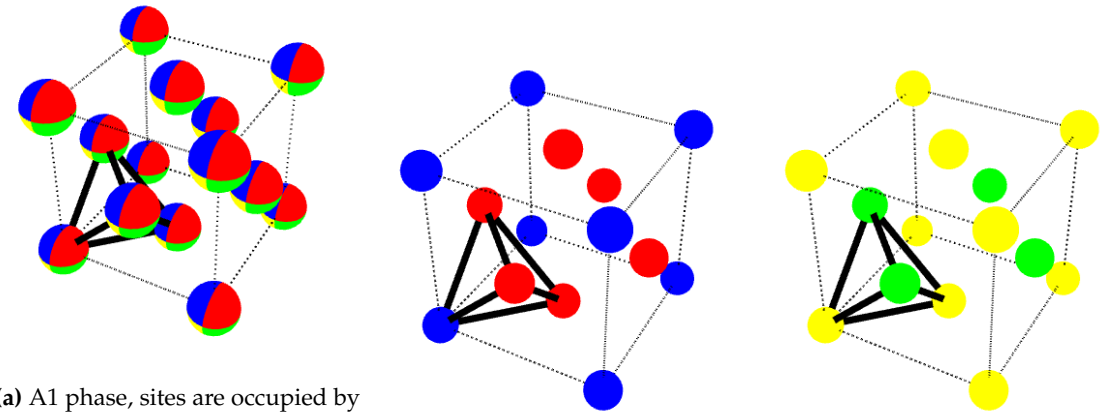

(a) A1 phase, sites are occupied by Cr, Mn, Fe, and Ni in probabilities determined by their average concentration in the system

(b) $L1_2$ phase corresponding to $CrFe_3$ with Cr and Fe

(c) $L1_0$ phase corresponding to MnNi with Mn and Ni

Figure 2. (a) Most probable phase at high temperature (disordered structure); (b) and (c): two most probable ordered phases at low temperature in the equiatomic $Cr_{25}Fe_{25}Mn_{25}Ni_{25}$ and $Cr_{18}Fe_{27}Mn_{27}Ni_{28}$ HEAs compositions. Cr, Fe, Mn and Ni are illustrated in blue, red, yellow and green respectively.

3.3. Origin of the high correlation functions Mn-Mn-Ni-Ni and Cr-Fe-Fe-Fe in the low temperature region

The symmetry unique decorations, (s), are generated by studying all of the decorations $(s)_{\omega_i,n_i}$ from the sub-clusters ω_i, n_i in ω, n that have decorations with empty cluster, i.e. at least one integer entry in $0 \subseteq (s)_{\omega_i,n_i}$. For example, in the case of a two-body cluster consisting of sites $\{(1,1,1),(1,3/2,3/2)\}$, see Tab. 1, we have $4^2 = 16$ 2-tuples of decorations. It can be noted that the cluster $\{(1,1,1),(1,3/2,3/2)\}$ contains two sub-clusters: the point cluster $\{(1,1,1)$ that has decorations $\{(0),(1),(2),(3)\}$ and the cluster itself which has decorations $\{(1,1),(2,1),(3,1),(2,2),(2,3),(3,3)\}$. In general any given sub-cluster ω_i, n_i can be contained several times inside the cluster ω, n. For example in this case the the point cluster is contained twice: one time in $(1,1,1) \subset \{(1,1,1),(1,3/2,3/2)\}$ and also in $(1,3/2,3/2)\{(1,1,1),(1,3/2,3/2)\}$; similarly the cluster itself $\{(1,1,1),(1,3/2,3/2)\}$ is contained just once. To transfer the sub-cluster decorations in notation ω_i tuples to ω tuples notation we make use of the empty cluster X. Thus a point cluster decorated by $(s) = (3)$ is transfered to ω tuples notation in the maximal cluster as $(3,0)$ or $(0,3)$; this can be captured by the permutation operators $\{(1,X),(X,1)\}$ (see Tab. 2) where X stands for empty cluster where a 0 should be placed. Similarly the ω tuples $(1,2)$ in the ω cluster notation are equivalent to $(1,2)$ and $(2,1)$, this can again be captured by permutation operators $\{(1,2),(2,1)\}$, where X no longer appears, since the ω_i tuples have the same order as the ω tuples.

The analysis otlined above for the two body cluster $\{(1,1,1),(1,3/2,3/2)\}$ with $K = 4$ components can be extended to larger clusters. The permutation operators that carry the appropriate decorations $(s)_{\omega_i,n_i}$ of sub-clusters ω_i, n_i into ω, n cluster ω tuples notation are detailed in Tab. 2. It should be noted that for any two body cluster, the point and corresponding pair sub-clusters add up forming $4+6=10$ symmetrically unique correlation functions $\langle \Gamma^{(ij)}_{\omega,n}[\vec{\sigma}] \rangle$.

In general the total number correlation functions K^ω required to describe a maximal cluster in the CE can be found by summing the total number of symmetrically unique decorations for all of the sub-clusters included in a given maximal cluster. The symmetry unique decorations for each of the sub-clusters is reported in ATAT clusters.out file and here it is summarized in the Tab. 1, and the particular sub-clusters included in a maximal cluster are listed in the Tab. 2. If the sub-cluster has $\omega_i < \omega$, then the decorations from the sub-cluster can be transferred into the decorations of the

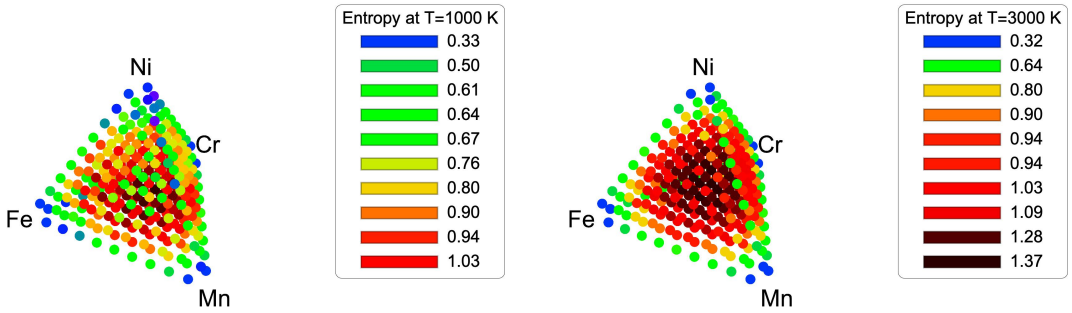

(a) Composition dependent entropy at fixed temperature 1,000 K

(b) The same as in (a) but at fixed temperature 3,000 K

Figure 3. Composition dependent entropies obtained from Monte Carlo simulations in CE.

maximal cluster by using the permutation operators in Tab. 2 including X for the empty site. For example, the cluster $(\omega = 3, n = 1)$ has 3 sub-clusters $(\omega_1 = 1, n_1 = 1)$, $(\omega_2 = 2, n_2 = 1)$ and $(\omega_3 = 3, n_3 = 1)$, the number of permutation operators associated with sub-cluster $(\omega_1 = 1, n_1 = 1)$ is 4; for $(\omega_2 = 2, n_2 = 1)$ we find 6 permutation operators; and for the cluster itself $(\omega_3 = 3, n_3 = 1)$ we find 6 permutation operators. The point sub-cluster $(\omega_1 = 1, n_1 = 1)$ has, according to Tab. 1, 4 decorations associated to it; the two body cluster $(\omega_2 = 2, n_2 = 1)$ has 6 decorations associated to itself; and finally the sub-cluster $(\omega_3 = 3, n_3 = 1)$ has 10 decorations associated to itself. On the other hand, the number of symmetrically unique correlation functions, which is smaller than K^ω, but can nevertheless fully describe cluster $(\omega = 3, n = 1)$ with $K = 4$ components is given by $4 + 5 + 10 = 19$ correlation functions. The remaining decorations 45 are obtained by using appropriately the $3 + 6 + 6 = 15$ permutation operators. Similarly maximal cluster $(\omega = 3, n = 2)$ has 34 symmetrically unique decorations and $(\omega = 4, n = 1)$ has 35 decorations.

The structure with configuration Mn-Mn-Ni-Ni can be understood as $L1_0$ in strukturbericht notation with Mn and Ni, similarly the structure with composition Cr-Fe-Fe-Fe can be understood as $L1_2$ in strukturbericht notation; both of these structures are depicted in Fig. 2. The entropy increase (Fig. 3) with temperature corresponding to the equiatomic alloy composition can thus be understood by the decrease in probabilities (Figs. 1) with temperature of the ordered states corresponding to the structures $L1_0$ towards the disorder configuration $A1$ (see Fig. 2 depicting this ordered structure and the disordered phase). Similarly, in the alloy with composition $Cr_{18}Fe_{27}Mn_{27}Ni_{28}$, the high probability of the configuration Cr-Fe-Fe-Fe is found to be correlated to the ordered structure $L1_2$-$CrFe_3$. In particular, the latter structure has been found to be stable due to the strong anti-ferromagnetic interaction between Cr and Fe from DFT calculations performed for the FeCrNi system [38]. In that work, Monte Carlo simulations using magnetic cluster expansion indicated that ordered magnetic structures in the Ni-rich corner (ferromagnetic) of the *FeCrNi* system persists until temperatures of 600 K, and that for the atomic compositions between $CrFe_2$ and $CrFe_3$ magnetic order (anti-ferromagnetic) was retained beyond 500 K. Similarly the structure $L1_0$-MnNi was found to be among the most stable intermetallic structures with the smallest enthalpy of mixing in the FeCrNi FCC system [39].

4. Configuration entropy in Cr-Fe-Mn-Ni system

Composition dependent entropies at fixed temperatures 1000 K and 3000 K are shown in Fig. 3 a-b. At each of these temperature values, any of the configuration entropy expressions from Tab. 2 provides approximately the same value. At 3000 K, the entropy is maximized in the center of the tetrahedron namely at the equiatomic composition to 1.37 k_B, and it is decreased upon lowering the

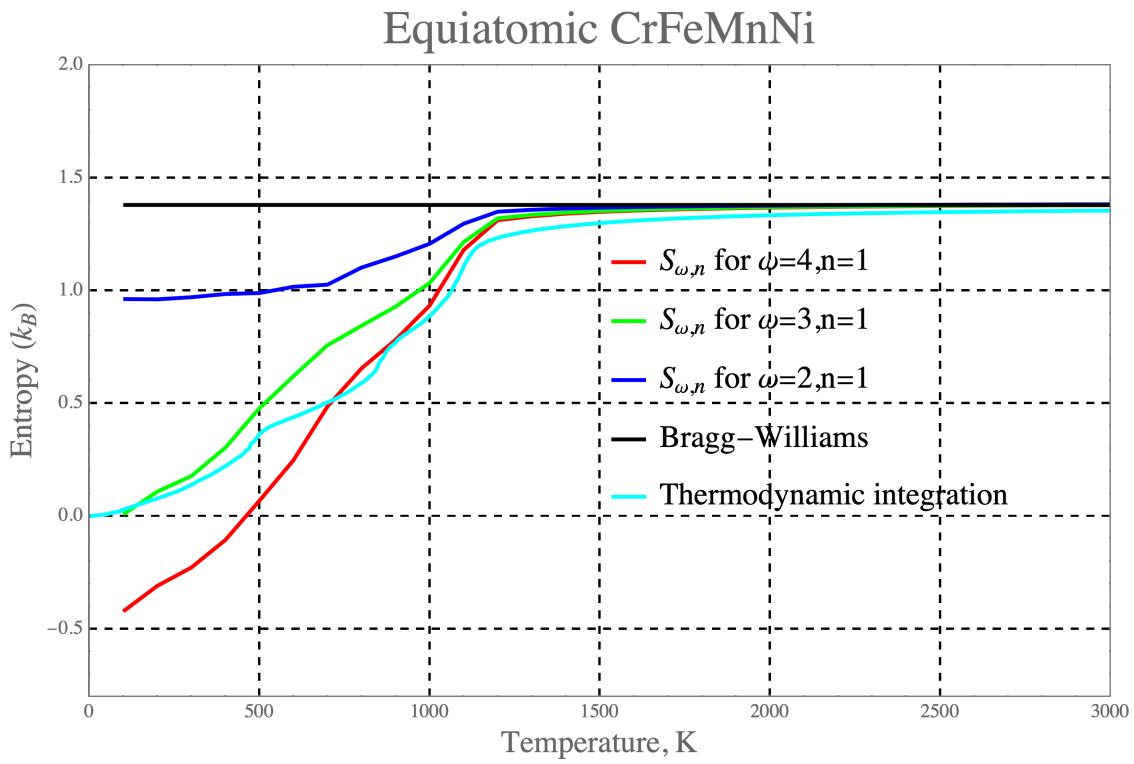

Figure 4. Temperature dependent entropy in equiatomic composition $Cr_{25}Fe_{25}Mn_{25}Ni_{25}$

temperature at all of the composition points. The variation of configuration entropy is too complex to be captured in the fixed temperature plots, therefore we use specifically the equiatomic composition and calculate the configuration entropy as a function of temperature in Fig. 4. Regarding the high temperature limit value of entropy Figs. 4 , we use as maximal cluster that from the four body, three body and two body in the nearest neighbor cluster probabilities. We see that at low temperatures, the entropy becomes slightly negative with respect the thermodynamic integration value, whilst the high temperature limit of disordered solid solution $-k_B \sum_p x_p[\vec{\sigma}] ln(x_p[\vec{\sigma}])$ is achieved faster than in the thermodynamic integration approximation. The reason the high temperature limit is preserved can be clearly seen from the factorization of the CE expression that resulted in Eq. 15.

5. Conclusions

The design of radiation tolerant materials for advanced nuclear reactor systems can be accelerated by using ab initio computational materials science. The composition $Cr_{18}Fe_{27}Mn_{27}Ni_{28}$ multicomponent system has been studied for advanced nuclear applications due to the removal of Co, which can cause activation by transmutation of ^{60}Co isotope during service in a nuclear reactor and promising irradiation resistance with regards to void swelling.

In this work we develop a matrix formalism to study multi-body ordering probabilities, SRO and configuration entropy. We apply our methods to the system CrFeMnNi for use in the CE. The cluster probabilities are worked out by explicit inversion and direct product of a matrix formulation obtained from symmetry independent correlation functions. The correlation functions are determined from semi-canonical Monte Carlo simulations and ECIs derived from DFT calculations. In particular, we apply our methods to the specific case of FCC CrFeMnNi HEA by considering 285 different alloy compositions covering the compositional space of the quaternary alloy as a function of temperature. To further assess our formulated expressions for configuration entropy, focus is put at two alloy compositions equiatomic $Cr_{25}Fe_{25}Mn_{25}Ni_{25}$ and $Cr_{18}Fe_{27}Mn_{27}Ni_{28}$ to obtain cluster probabilities and understand the variation in configuration entropy with temperature due to the lowering the

ordering probability corresponding to the ordered configuration. The cluster probability plots against temperature show that for the composition $Cr_{18}Fe_{27}Mn_{27}Ni_{28}$ there is high probability of formation of the $L1_0$ MnNi phase at low temperatures below 1300 K and for the $L1_2$ $CrFe_3$ phase in the temperature range 500-1200 K. Similarly for the equiatomic composition the $L1_0$ MnNi phase appears stable in the temperature range 900-1200 K, while the lower temperature region is preferred for the configuration Cr-Fe-Mn-Ni. The configuration Cr-Cr-Cr-Cr was found to be the least probable configuration at all temperature ranges for both compositions of the Cr-Fe-Mn-Ni system. Furthermore, configuration entropy as a function of temperature was derived from these probabilities: the high-temperature limit is in accordance with random solid solution approximation; but at low temperatures, the entropy is seen to be reduced due to ordering or segregation tendencies.

Acknowledgments: This work has been carried out within the framework of the EUROfusion Consortium and has received funding from the Euratom research and training programme 2014-2018 under Grant Agreement No. 633053 and funding from the RCUK Energy Programme [Grant Number EP/P012450/1]. The views and opinions expressed herein do not necessarily reflect those of the European Commission. AFC acknowledges financial support from EPSRC (EP/ L01680X/1) through the Materials for Demanding Environments Center for Doctoral Training. MF and JSW acknowledge the financial support from the Foundation of Polish Science grant HOMING (No.Homing/2016-1/12). The HOMING programme is co-financed by the European Union under the European Regional Development Fund. The simulations were partially carried out by MF with the support of the Interdisciplinary Centre for Mathematical and Computational Modelling (ICM), University of Warsaw, under grant no GA65-14. DNM acknowledges the support from high-performace computing facility MARCONI (Italy) provided by the EUROfusion.

Author Contributions: AFC and DNM developed theoretical formalism and applied the formulation to the CrFeMnNi system. AFC, DNM and JSW wrote the manuscript and PMM checked grammar. JSW and MF provided the results of DFT-based semi canonical Monte Carlo simulations for CrFeMnNi system. All the authors made comments into the final version before its submission.

Conflicts of Interest: The authors declare no conflict of interest.

Abbreviations

The following abbreviations are used in this manuscript:

CE: Cluster Expansion
CVM: Cluster Variation Method
HEA: High-Entropy Alloy
K: Number of components in alloy
DFT: Density Functional Theory
GS: Ground States
G: Space Group of the disordered high temperature structure
(ω_i, n_i): i^{th} sub-cluster of a maximal cluster (ω, n)
$\mathcal{N}_{\omega_i,n_i}$: operators $g \in G$ acting on the sites of cluster (ω_i, n_i) to rearrange the sites i.e. a permutation
N_{ω_i,n_i}: site multiplicity of the cluster ω_i
$N^{\beta}_{\omega,n}$: sub-cluster multiplicity of the cluster $\beta \in (\omega, n)$
$\Omega[\omega, n]$: Number of times a cluster ω, n is contained in a supercell structure, generally used for Monte Carlo simulations, for obtaining thermodynamic quantities.

Bibliography

1. Cantor, B.; Chang, I.; Knight, P.; Vincent, A. Microstructural development in equiatomic multicomponent alloys. *Materials Science and Engineering A* **2004**, *375-377*, 213–218.
2. Yeh, J.W.; Chen, S.K.; Lin, S.J.; Gan, J.Y.; Chin, T.S.; Shun, T.T.; Tsau, C.H.; Chang, S.Y. Nanostructured High-Entropy Alloys with Multiple Principal Elements: Novel Alloy Design Concepts and Outcomes. *Advanced Engineering Materials*, *6*, 299–303.
3. Gali, A.; George, E.P. Tensile properties of high- and medium-entropy alloys. *Intermetallics* **2013**, *39*, 74–78.

4. Carroll, R.; Lee, C.; Tsai, C.W.; Yeh, J.W.; Antonaglia, J.; Brinkman, B.A.W.; Leblanc, M.; Xie, X.; Chen, S.; Liaw, P.K.; Dahmen, K.A. Experiments and Model for Serration Statistics in Low-Entropy, Medium-Entropy, and High-Entropy Alloys. *Scientific Reports* **2015**, *5*, 16997.
5. Xia, S.; Gao, M.C.; Yang, T.; Liaw, P.K.; Zhang, Y. Phase stability and microstructures of high entropy alloys ion irradiated to high doses. *Journal of Nuclear Materials* **2016**, *480*, 100–108.
6. Lucas, M.S.; Mauger, L.; Muñoz, J.A.; Xiao, Y.; Sheets, A.O.; Semiatin, S.L.; Horwath, J.; Turgut, Z. Magnetic and vibrational properties of high-entropy alloys. *Journal of Applied Physics* **2011**, *109*, 07E307.
7. Calvo-Dahlborg, M.; Cornide, J.; Tobola, J.; Nguyen-Manh, D.; Wróbel, J.S.; Juraszek, J.; Jouen, S.; Dahlborg, U. Interplay of electronic, structural and magnetic properties as the driving feature of high-entropy CoCrFeNiPd alloys. *J. Phys. D. Appl. Phys.* **2017**, *50*, 185002.
8. Rossiter, P.L.; Wells, P. The dependence of the electrical resistivity on short-range order. *Journal of Physics C: Solid State Physics* **1971**, *4*, 354 – 363.
9. Spruiell, J.E.; Stansbury, E.E. X-Ray study of short-range order in nickel alloys containing 10.7 and 20.0 at. % Molybdenum. *Journal of Physics and Chemistry of Solids* **1965**, *26*, 811–822.
10. Fisher, J.C. On the strength of solid solution alloys. *Acta Metallurgica* **1954**, *2*, 9–10.
11. Fernández-Caballero, A.; Wróbel, J.S.; Mummery, P.M.; Nguyen-Manh, D. Short-Range Order in High Entropy Alloys: Theoretical Formulation and Application to Mo-Nb-Ta-V-W System. *Journal of Phase Equilibria and Diffusion* **2017**, *38*, 391–403.
12. Santodonato, L.J.; Zhang, Y.; Feygenson, M.; Parish, C.M.; Gao, M.C.; Weber, R.J.K.; Neuefeind, J.C.; Tang, Z.; Liaw, P.K. Deviation from high-entropy configurations in the atomic distributions of a multi-principal-element alloy. *Nature communications* **2015**, *6*, 5964.
13. Leong, Z.; Wróbel, J.S.; Dudarev, S.L.; Goodall, R.; Todd, I.; Nguyen-Manh, D. The Effect of Electronic Structure on the Phases Present in High Entropy Alloys. *Scientific Reports* **2017**, *7*, 39803.
14. Van de Walle, A. Multicomponent multisublattice alloys, nonconfigurational entropy and other additions to the Alloy Theoretic Automated Toolkit. *Calphad: Computer Coupling of Phase Diagrams and Thermochemistry* **2009**, *33*, 266–278.
15. Lu, Z.W.; Wei, S.H.; Zunger, A.; Frota-Pessoa, S.; Ferreira, L.G. First-principles statistical mechanics of structural stability of intermetallic compounds. *Physical Review B* **1991**, *44*, 512–544.
16. Lechermann, F.; Fähnle, M.; Sanchez, J.M. First-principles investigation of the Ni-Fe-Al system. *Intermetallics* **2005**, *13*, 1096–1109.
17. Ackermann, H.; Inden, G.; Kikuchi, R. Tetrahedron approximation of the cluster variation method for b.c.c. alloys. *Acta Metallurgica* **1989**, *37*, 1–7.
18. Tepesch, P.D.; Asta, M.; Ceder, G. Computation of configurational entropy using Monte Carlo probabilities in cluster-variation method entropy expressions. *Modelling and Simulation in Materials Science and Engineering* **1998**, *6*, 787–797.
19. Kumar, N.K.; Li, C.; Leonard, K.; Bei, H.; Zinkle, S. Microstructural stability and mechanical behavior of FeNiMnCr high entropy alloy under ion irradiation. *Acta Materialia* **2016**, *113*.
20. Hart, G.L.W.; Forcade, R.W. Algorithm for generating derivative structures. *Physical Review B - Condensed Matter and Materials Physics* **2008**, *77*.
21. Cenedese, P.; Gratias, D. Multicomponent formalism in the mean-field approximation: a geometric interpretation of Chebychev polynomials. *Physica A: Statistical Mechanics and its Applications* **1991**, *179*, 277–287.
22. Sluiter, M.H.; Kawazoe, Y. Invariance of truncated cluster expansions for first-principles alloy thermodynamics. *Physical Review B - Condensed Matter and Materials Physics* **2005**, *71*, 1–2.
23. Blum, V.; Zunger, A. Prediction of ordered structures in the bcc binary systems of Mo, Nb, Ta, and W from first-principles search of approximately 3,000,000 possible configurations. *Physical Review B - Condensed Matter and Materials Physics* **2005**, *72*, 3–6.
24. Finel, A. The cluster variation method and some applications. In *Proceedings of NATO Advanced Study Institute on Statics and Dynamics of Alloy Phase Transformations*; Turchi, P.E.A.; Gonis, A., Eds.; Springer: Rhodes, Greece, 1992; pp. 495–540.
25. Kikuchi, R. A Theory of Cooperative Phenomena. *Physical Review* **1951**, *81*, 988–1003.
26. Barker, J.A. Methods of Approximation in the Theory of Regular Mixtures. *Proceedings of the Royal Society A: Mathematical, Physical and Engineering Sciences* **1953**, *216*, 45–56.

27. Gratias, D.; Sanchez, J.; De Fontaine, D. Application of group theory to the calculation of the configurational entropy in the cluster variation method. *Physica A: Statistical Mechanics and its Applications* **1982**, *113*, 315–337.
28. Van de Walle, A.; Asta, M. Self-driven lattice-model Monte Carlo simulations of alloy thermodynamic properties and phase diagrams. *Modelling and Simulation in Materials Science and Engineering* **2002**, *10*, 521–538.
29. Wróbel, J.S.; Nguyen-Manh, D.; Kurzydłowski, K.J.; Dudarev, S.L. A first-principles model for anomalous segregation in dilute ternary tungsten-rhenium-vacancy alloys. *Journal of Physics: Condensed Matter* **2017**, *29*, 145403.
30. Blöchl, P.E. Projector augmented-wave method. *Phys. Rev. B* **1994**, *50*, 17953–17979.
31. Kresse, G.; Hafner, J. Ab initio molecular-dynamics simulation of the liquid-metal–amorphous-semiconductor transition in germanium. *Phys. Rev. B* **1994**, *49*, 14251–14269.
32. Kresse, G.; Joubert, D. From ultrasoft pseudopotentials to the projector augmented-wave method. *Phys. Rev. B* **1999**, *59*, 1758–1775.
33. Kresse, G.; Hafner, J. Ab initio molecular dynamics for liquid metals. *Phys. Rev. B* **1993**, *47*, 558–561.
34. Kresse, G.; Furthmüller, J. Efficient iterative schemes for ab initio total-energy calculations using a plane-wave basis set. *Phys. Rev. B* **1996**, *54*, 11169–11186.
35. Kresse, G.; Furthmüller, J.; Furthmiiller B ', J. Efficiency of ab-initio total energy calculations for metals and semiconductors using a plane-wave basis set. *Comput. Mater. Sci.* **1996**, *6*, 15–50.
36. Perdew, J.P.; Burke, K.; Ernzerhof, M. Generalized Gradient Approximation Made Simple. *Phys. Rev. Lett.* **1996**, *77*, 3865–3868.
37. Monkhorst, H.J.; Pack, J.D. Special points for Brillouin-zone integrations. *Phys. Rev. B* **1976**, *13*, 5188–5192.
38. Lavrentiev, M.Y.; Wróbel, J.S.; Nguyen-Manh, D.; Dudarev, S.L.; Ganchenkova, M.G. Magnetic cluster expansion model for random and ordered magnetic face-centered cubic Fe-Ni-Cr alloys. *J. Appl. Phys.* **2016**, *120*, 043902.
39. Wróbel, J.S.; Nguyen-Manh, D.; Lavrentiev, M.Y.; Muzyk, M.; Dudarev, S.L. Phase stability of ternary fcc and bcc Fe-Cr-Ni alloys. *Phys. Rev. B* **2015**, *91*, 024108.